

Four Decades of Progress in Monitoring and Modeling of Processes in the Soil-Plant-
Atmosphere System: Applications and Challenges

A stochastic texture-based approach for evaluating solute
travel times to groundwater at regional scale by coupling GIS
and transfer function

A. Coppola^{a*}, A. Comegna^b, G. Dragonetti^c, L. De Simone^b, N. Lamaddalena^c, P.
Zdruli^c, A. Basile^d

^aDepartment of European and Mediterranean Cultures-Architecture, Environment, Cultural Heritage (DICEM), Hydraulics and Hydrology Division, University of Basilicata, Matera, 75100, Italy (E-mail address: antonio.coppola@unibas.it)

^bSchool of Agricultural Forestry, Food and Environmental Sciences (SAFE), University of Basilicata, Potenza, 85100, Italy

^cInstitute for Mediterranean Agricultural and Forestry Systems, National Research Council (CNR), Ercolano (NA), 80056, Italy

^dMediterranean Agronomic Institute, Land and Water Division, IAMB, Bari, 70010, Italy

Abstract

Interpreting and predicting the evolution of non-point source (NPS) pollution of soil and surface and subsurface water from agricultural chemicals and pathogens, as well as overexploitation of groundwater resources at regional scale are continuing challenges for natural scientists. The presence and build up of NPS pollutants may be harmful for both soil and groundwater resources. Accordingly, this study mainly aims to developing a regional-scale simulation methodology for groundwater vulnerability that use real soil profiles data. A stochastic approach will be applied to account for the effect of vertical heterogeneity on variability of solute transport in the vadose zone. The approach relies on available datasets and offers quantitative answers to soil and groundwater vulnerability to non-point source of chemicals at regional scale within a defined confidence interval. The study area is located in the Metaponto agricultural site, Basilicata Region-South Italy, covering approximately 12000 hectares. Chloride will be considered as a generic pollutant for simulation purposes. The methodology is based on three sequential steps: 1) designing and building of a spatial database containing environmental and physical information regarding the study area, 2) developing travel time distributions for specific textural sequences in the soil profile, coming from texture-based transfer functions, 3) final representation of results through digital mapping. Distributed output of soil pollutant leaching behavior, with corresponding statistical uncertainties, will be visualized in GIS maps. Of course, this regional-scale methodology may be extended to any specific pollutants for any soil, climatic and land use conditions.

* Corresponding author. Tel.: +39-0971-209-169
E-mail address: antonio.coppola@unibas.it

© 2013 The Authors. Published by Elsevier B.V
Selection and/or peer-review under responsibility of the Scientific Committee of the conference

Keywords: Non-Point Source pollution; Solute Transfer Function; GIS modeling; stochastic modeling.

1. Introduction

Chemical-microbial pollution of soils and subsurface water resources is the consequence of many human activities among which agriculture is certainly one of the most important [1]. Accordingly, protection of soils and subsurface water resources should be among the highest priorities of our society, owing to the reliance upon of these resources as a supply for drinking (water) and agriculture uses (soil and water). This has strongly attracted the public attention upon the need to protect soils and groundwater resources from non-point source pollutants. The protection and sustainability of soil and water resources can only be assured through a better understanding of vadose zone processes at different spatio-temporal scales. Unfortunately, outstanding progress of the recent years in understanding the role of the unsaturated zone have frequently been limited to relatively small spatio-temporal scales. Indeed, storage, redistribution, transport and transformation processes of water and chemicals are understood for limited-scale systems. Major progresses have been achieved through parallel studies aiming to set up monitoring techniques [2] as well as modeling tools [3; 4]. A local-field-scale knowledge now exists about the occurrence of complex physical phenomena inducing preferential flow paths, whose size and assemble depend on the porous medium physical-chemical characteristics, which may reduce or enhance the mobility of water and pollutants [5; 6]. What's more, studies also exists on how the contamination process may be enhanced by the presence of colloids which act as pollutants carriers [7; 8]. To the contrary, a principal challenge for the scientific community in the recent years has remained how to apply our physical-hydrological understanding across scales [9; 10; 11; 12; 13]. Knowledge gaps still remain in transfer across spatio-temporal scales, and multidisciplinary integration of results. The knowledge and information required to address the problem of NPS pollutants in the vadose zone cross several technological and sub disciplinary lines: spatial statistics, geographic information systems (GIS), hydrology, soil science, and remote sensing [14; 15]. As discussed by Stewart [16], the main issues encountered by NPS groundwater vulnerability assessment, are the large spatial scales, the complex processes that govern fluid flow and solute transport in the unsaturated zone, the absence of unsaturated zone measurements of diffuse contaminant concentrations in 3-D regional-scale space as these are difficult, time consuming, and prohibitively costly, and the computational effort required for solving the nonlinear equations for physically-based modeling of regional scale, heterogeneous applications [15]. This results in significant simplifying assumption in NPS agrochemical leaching models.

Currently, existing regional-scale leaching models can be grouped into four main categories, ranging from qualitative models that rely on index and overlay techniques, over simple drainage algorithms, to stream tube models, and process-based numerical simulations [15].

Following the approach proposed by Stewart and Loague, here is presented a methodology that is based on coupling of transfer function and GIS modeling. The methodology represents the result of the up-scaling procedure applied to Jury's Transfer Function Model (TFM) [3]. A texture-specific transfer function is developed providing texture-based travel time probability density functions and describing a characteristic leaching behavior for soil profiles. The latter, in turn, have to be estimated by indirect estimations techniques such as pedo-transfer functions (PTFs) [17; 18], to overcome the trouble of intensive in situ and/or laboratory determinations of soil hydraulic and hydrodispersive properties, which are generally lacking for regional scale studies. Some researchers [19; 20] proved the point of regional specificity and remarked the impacts of soil and climatic conditions on the PTF predictions reliability.

This is also our view. This is why in our study we developed area-specific pedotransfer functions based on our own texture-hydraulic properties datasets coming from several sites in the investigated area.

GIS, besides, will be used here as a spatially database management system that is able to depict real world soil, climatic and groundwater features of relevance to the leaching process, serving both as a baseline data depot for hydraulic modeling and a final gateway for output representation and interactive delivery. A preliminary evaluation of methodology will be carried out by applying it to quantify solute transport in the Metaponto plain in Southern Basilicata, Italy. A wide area (about 12000 ha) was completely characterized by a pedological point of view by digging several soil profiles. The textural properties of soil horizons of each soil profile were converted to the corresponding hydraulic properties by using a PTF specifically calibrated for the soils of the area (mainly silty-loam, silty and silty clay).

2. Materials and methods

2.1. Study area

The area of interest was the sub-basin of Metaponto agricultural site, located in southern Basilicata, Italy, approximately 11698 hectares in size and crossed by two main rivers, Sinni and Agri, and from many secondary water bodies. Figure 1 shows the location of the study area.

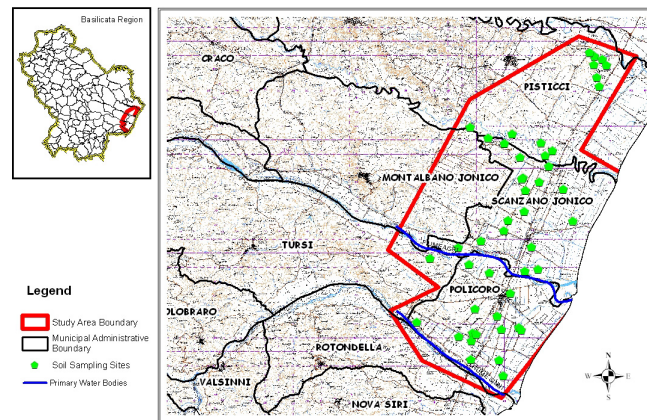


Fig. 1. Study area.

Topographically, the area is characterized by fairly distinct variations in elevation in the western part of the basin, away from the coast, and extremely flat terrain in the near-shore portions of the basin, to the south and east. Much of the basin is used for agricultural purposes. Major crops and land uses receiving applications of nutrients and chemicals include cereals, vegetables, fruit orchards. Soils that support these land uses range from the loam to clay loam, in the northern portions of the basin, to the fine silty loams in the southern basin.

2.2. Geo Database implementation

2.2.1. Land Use

Land use dataset, published within PROGETTO SIGRIA, INEA 2000, was used to describe cropped species at parcel level, and furthermore to define the spatial extent of the whole GIS project in this work. Table 1 shows cropped surfaces in hectares summarized by aggregated land use classes. Fruit orchards

cover almost 44% of total study area, followed by ploughed areas covering 15%, vegetables 10% and cereals 10%. Non vegetated areas, such as urban or water bodies make up for 15%.

Table 1. Land Use Classes.

Land use	Number of parcels	Hectares
Non vegetated area	1505	17.705
Forest	10	0.524
Cereal	445	10.794
Fruit tree	1689	50.564
Leguminous	39	0.624
Olive orchard	456	4.206
Vegetable	1003	10.959
Grass land and pasture	16	0.660
Ploughed areas	1083	17.816
Grape orchard	229	3.131

2.2.2. Soil Texture

Laboratory analysis data were originally acquired from regional geology agency in tabular format for 52 soil profiles sampled across the study area. For simplifying input data interpolation at regional scale, in this study a fictitious soil system was adopted assuming the soil to be composed of only two layers, A and B, the first being superficial and 40 centimeters thick (this was the average depth of the first horizon for all the soil profiles, and the latter reaching the water table). A fictitious soil profile was obtained for each real soil profile by averaging textural data with a weighted procedure using horizon depths as weights. Data were then imported into GIS and spatial structure of Sand, Clay, Silt contents and Depth measures was analyzed with Exploratory Spatial Data Analysis (ESDA) tools, by means of classic statistical analysis, QQ plot, Trend analysis, and Semivariogram-Crossvariance cloud analysis. In consideration of ESDA investigation, variables for each soil layer, were then interpolated with kriging model. As a result, continuous surfaces for sand, clay, silt, and soil profile depth were produced in raster format for both A and B soil layers (maps not shown).

Sand, Silt and Clay raster datasets were concurrently queried with a map calculator using a set of SQL statements, each defining a texture constraint for each soil class according to USDA classification system, in order to produce two final texture maps (Figure 2) one for each fictitious soil layer.

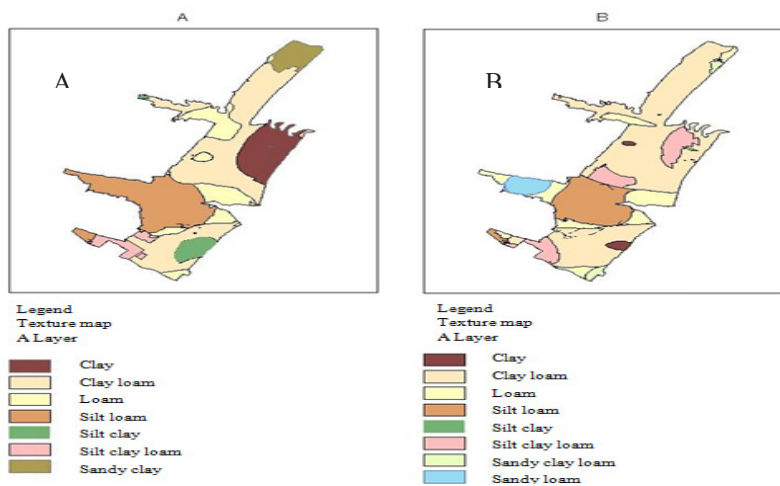


Fig. 2. Texture map for layers A and B.

Table 2 shows texture classes for each soil layer, along with corresponding areas. Clay loam is the predominant class in both layers.

Table 2. Texture classes for each layer soil.

	Texture classes			
	Layer A		Layer B	
	Hectares	% of study area	Hectares	% of study area
Clay	1353.806	11.57	125.35	1.07
Clay loam	4744.788	40.56	6624.283	56.63
Loam	1624.41	13.89	1500.709	12.83
Sandy clay	590.091	5.04		
Silt clay	422.327	3.61	10.296	0.09
Silt clay loam	373.314	3.19	1102.732	9.43
Silt loam	2589.581	22.14	1786.111	15.27
Sandy clay loam			160.872	1.38
Sandy loam			387.198	3.31

2.2.3. Precipitation, Temperature and Evapotranspiration

Climate data on a daily basis for the 1999-2009 period for all the climatic stations localized in the area of interest are shown in table 3 and were provided by Regional Agriculture Services.

Table 3. Climate data for the period 1999-2009

ALSIA climatic station	Average Temp. (°C)	Average rainfall (mm)	n. observation years
Tursi c.da Marone	17.28	555.20	10
Montalbano c.da Fico	16.01	450.45	10
Novasiri farm “La collinetta”	17.24	529.38	10
Pisticci c.da Castelluccio	16.41	423.07	10
Pisticci c.da Paolona	16.05	469.02	10
Policoro c.da Troly	15.90	470.93	10
Policoro loc. Wood Sottano	15.90	470.93	10
Metaponto farm “Pantanello”	17.15	505.89	9

The “Voronoi algorithm” was used for spatial partitioning of the study area according to the “spheres of influence” of each rainfall station.

2.2.4. Elevation

Contour lines on IGM 1:5.000 base maps were digitized, a triangulated irregular network was created from them and finally converted into a raster dataset. From elevation grid, slope grid was derived as well.

2.2.5. Depth to Groundwater

DITEC department of University of Basilicata provided tabular data for 192 measuring wells, 51 of which were located within the study area. Once imported into GIS as a point feature dataset, groundwater depth at measuring stations was interpolated using Kriging, thus resulting in a continuous surface (map not shown).

2.3. Geo Database and data manipulation

So far vector and raster datasets were collected, each carrying spatially distributed information. At this point GIS must provide hydrologic modeling with a spatial database carrying all the necessary information for leaching assessment: texture class, soil depth, water table depth, and net water recharge.

In order to achieve such goal, data were aggregated at homogenous soil units level on one common layer enabling, therefore further data manipulation and derived variables creation. Homogenous soil units, being areas characterized by sufficiently similar leaching behavior, were defined intersecting soil texture information for layers A and B through geoprocessing tools finally resulting in a polygon feature vector dataset, each polygon defining a combination of two overlaying texture classes. Overall, 31 possible texture combinations classes were found. Finally zonal attribute transfer was then performed from land use, rain, freaticmetry, temperature, slope, and elevation datasets to soil unit feature dataset, in order to associate to each soil unit such spatially distributed information averaged for each polygon surface. Furthermore for each soil unit potential evapotranspiration (ETp) was calculated using the Thornthwaite formula. At this point the spatial database was set up with all calculated physical attributes related to each polygon representing an homogeneous soil unit. As an example, table 4 shows three explanatory records. Such database was used as input in the leaching model as discussed in the following section.

Table 4. Spatial database for three explanatory records.

Polygon	Texture overlay	Land use	Mean	Mean depth of	Annual mean	Annual net
1	Clay loam on Clay	Fruit tree	0.628	26.238	900	623
2	Clay loam on Clay loam	Olive orchard	0.611	15.682	1099	1261
3	Clay loam on Clay loam	Fruit tree	0.595	11.024	988	1340

3. Stochastic generation of texture-based solute transfer functions

3.1 Texture-based hydraulic and solute travel time distributions

In this study we assumed that the soil hydraulic properties can be described by the unimodal van Genuchten-Mualem model [21; 22] :

$$S_e = \frac{\theta - \theta_r}{\theta_0 - \theta_r} = \left[1 + |\alpha_{VG} h|^n \right]^{-m} \quad h < 0 \quad (1)$$

$$\theta = \theta_s \quad h \geq 0$$

$$K_r(S_e) = \frac{K(S_e)}{K_0} = S_e^\tau \left[1 - \left(1 - S_e^{1/m} \right)^m \right]^2 \quad (2)$$

In equation 1 S_e is effective saturation, α_{VG} (cm⁻¹), n and $m=1-1/n$ are shape parameters, θ_0 and θ_r are the saturated and residual water content, respectively. In equation 2, K_r is the relative hydraulic conductivity, τ is a parameter which accounts for the dependence of the tortuosity and the correlation factors on the water content and K_0 is the saturated hydraulic conductivity. A large dataset of hydraulic properties was already available for the textural classes of the area. They were measured in the laboratory on undisturbed soil samples (490 samples) collected at the soil surface during several previous measurement campaigns. For each soil sample a detailed particle-size distribution (PSD) was also available. PSD data were used as a basis for estimating soil water retention (and the corresponding parameters in equation 1) of soil horizons of each of the observation soil profiles by using the physico-

empirical PTF approach proposed by Arya and Paris [23]. Hereafter, such an approach will be referred to as the A&P approach.

The originally developed A&P model was refined by Basile and D'Urso [24] and Arya et al. [25], suggesting improvements pertaining to the limited flexibility of the original formulation. The original formulation based on a single optimization parameter (α_{AP}) was thus made more flexible by assuming a variable $\alpha_{AP}(h)$ with the pressure head h . Arya et al. [26] also derived an expression to compute $K(\theta)$ directly from the PSD, based on the same soil structure model leading to the $\theta(h)$ function [23; 25]. We opted for using the method only for estimating the saturated hydraulic conductivity. The whole hydraulic conductivity curve was estimated by using equation 2, with retention parameters and K_0 estimated by the A&P method and setting $\tau=0.5$. A specific $\alpha_{AP}(h)$ curve was obtained for each of the textural classes present in the investigated area. The measured hydraulic properties were partly (200 samples) used for the PTF calibration, by keeping the remaining data for the PTF validation.

In synthesis, a complete set of hydraulic parameters (θ_0 , θ_r , αVG , n , K_0 , $\tau=0.5$), estimated by a site-specific PTF, was available for all the textural classes found in the area. A Kolmogorov-Smirnov test showed that all the parameters were normally distributed. The means and the covariance matrix for the five parameters (all but τ) were computed for each of the textural classes encountered along the soil profiles. Thus, random field of the five parameters were produced with a Monte Carlo procedure from the correlated multivariate normal distribution for any textural classes by generating a vector x of independent standard normal deviates and then applying a linear transformation of the form $x=\mu+Lr_n$, where μ is the desired vector of means and L is the lower triangular matrix derived from the symmetric covariance matrix $V=LL^T$ decomposed by Cholesky factorization. In other words, the procedure generated random field with correlated parameters by multiplying the lower triangular Cholesky decomposition of the covariance matrix with vectors, r_n , containing five $N(0,1)$ randomly distributed numbers and by summing up the result to the mean of the parameters [27]. As pointed out by Smith and Diekkruger [28], using the statistical moments of the parameters of the hydraulic functions for generating the random field to be used in Monte Carlo simulations implies the assumption that soil hydraulic variability can be described by the statistical distribution of such parameters. This widely used approach is conceptually simple and is based on the idea of approximating stochastic processes by a large number of equally probable realizations. In this study, 400 sets of equally probable hydraulic parameter realizations were generated for each of the textural classes.

In order to simulate solute transport, dispersivity, λ , values have generally to be available for any soil horizons of a soil profile. As there were only limited measurements in the dataset for the area under study, we opted for deriving solute travel times distributions by applying the method proposed by Scotter and Ross [29], which deduces breakthrough curves of a tracer at a given depth for a given soil starting by the hydraulic conductivity function of that soil. According to the transfer function model (TFM) proposed by Jury and Roth [3], the flux concentration at a depth z , $C^f(z, I)$, given a time-varying flux concentration at the input surface $C^f(0, I)$ is given by:

$$C^f(z, I) = \int_0^I C^f(0, I - I') f^f(z, I) dI' \quad (3)$$

where $f^f(z, I)$ is the steady state travel time distribution (travel time pdf) defining the changes in the normalized concentration in the drainage as the cumulative drainage I builds up. For steady state flow conditions $I=qt$, where q is the steady state flow rate and t is the time. Scotter and Ross [29] assumed a gravity-induced water flow, a conservative and nonreactive solute and a purely convective flow, thus ignoring any convective mixing of solute flowing at different velocities and the effects of molecular diffusion. With these assumptions, the $f^f(z, t=I/q)$ for a pulse input of solute can be obtained as:

$$f^f(z, t) = \frac{dC^f(z, t)}{dt} = \frac{-1}{q} \frac{dK(\theta)}{dt} \quad (4)$$

where $K(\theta)$ is the hydraulic conductivity function which in this paper was assumed to be described by the van Genuchten-Mualem model (equations 1-2).

For a lognormal distribution of the cumulative drainage (or of travel times) the analytical expression for the pdf is a log-normal density function [3]:

$$f(I) = \frac{1}{\sqrt{2\pi}\sigma I} \exp\left[-\frac{(\ln I - \mu)^2}{2\sigma^2}\right] \quad (5)$$

in which μ and σ are the parameters of the log-normal pdf.

For the case of a stochastic-convective with log-normal distribution of travel times (CLT) model, if the $f^f(z, I)$ is known at a given depth z_1 than the TFM model allows for scaling that pdf to a depth z_2 according to the equation:

$$f^f(z_2, I) = \frac{z_1}{z_2} \left(z_1, I \frac{z_1}{z_2} \right) \quad (6)$$

This means that $\sigma_{z1} = \sigma_{z2}$ and $\mu_{z2} = \mu_{z1} + \ln(z_2/z_1)$. If, to the contrary, the transport process obeys to the Advection-Dispersion (AD) model, $\sigma_{z2} = \sigma_{z1}(z_1/z_2)^{0.5}$ and $\mu_{z2} = \mu_{z1} + \ln(z_2/z_1) + 0.5\sigma_{z1}^2(1 - z_1/z_2)$.

For each of the hydraulic parameter random vectors obtained for each textural classes, a corresponding fictitious breakthrough curve, $f^f(z, I)$, at an arbitrary depth $z=40$ cm was calculated according to the equation 4 for a solute pulse injection at the surface. An inert, non-adsorbed (a tracer) solute was selected for simulation purposes. In order to calculate the cumulative drainage I , an hourly inflow rate was calculated by assuming that all the net recharge (the rainfall infiltrated in the soil minus the evapotranspiration), was uniformly distributed over the year and that storage and surface runoff were negligible. By simply averaging over the 400 simulated breakthrough curves $f^f(z, I)$, an upscaled probability density function was obtained. Effective parameters μ (μ_{ef}) and σ (σ_{ef}) at 40 cm for each textural classes were estimated by fitting equation 5 to the upscaled curve.

3.2. Upscaled solute travel times distribution for textural sequences

By assuming the independence between two successive layers along a textural profile, assumed to consist of two layers, the mean $E(I, z=80$ cm) and variance $VAR(I, z=80$ cm) were obtained by summing up the $E(I, z=40$ cm) and $VAR(I, z=40$ cm) of the two textural classes for any textural sequence [30]. The $E(I, z)$ and the $VAR(I, z)$ were calculated as:

$$\begin{aligned} E(I, z) &= \exp(\mu_z + 0.5\sigma_z^2) \\ VAR(I, z) &= \exp(2\mu_z + \sigma_z^2) [\exp(\sigma_z^2) - 1] \end{aligned} \quad (7)$$

Once the upscaled 80 cm pdf was obtained, it was scaled with depth down to the water table according to the following hypothesis:

1. Two layers soil profile-the transport mechanism in the second layer down to the water table is the CLT (the effective parameters were scaled according to the CLT model);
2. Two layers soil profile-the transport mechanism in the second layer down to the water table is the CDE (the effective parameters were scaled according to the CDE model).

4. Results and discussion

Simulation results from the texture-based travel times distributions are synthesized in output maps as shown in figures 3a and 3b. The figures show the modal travel times for each textural sequences. Note the large discrepancies between peak travel times when the CD and the CLT processes are alternatively assumed, though the models provided the same average convective motion. Remarkable differences may be observed in travel time estimations for the same soil texture classes due to the underlying transport approaches and soil layer conceptualizations.

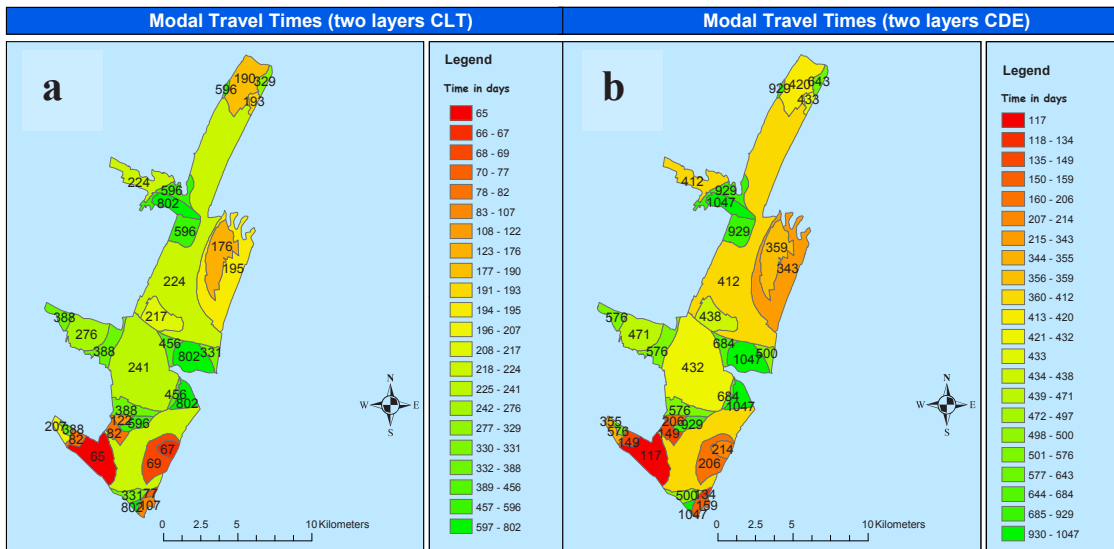


Fig. 3(a) Modal travel times map for CLT process; (b) Modal travel times map for and CDE process.

Generally CDE approach travel time values are higher than CLT ones by an average of 88%, a minimum of 30% (Loam on Loam) and a maximum of 220% difference (Silty Clay on Clay), while for one layer modality, differences result in slightly higher values. Highly vulnerable areas, obviously being characterized by a shorter travel time, depending on the travel modality compared to relatively more protected areas. Referring to CDE double layer modality, travel times values were reclassified using natural breaks classification method into three main vulnerability classes: low risk, medium risk and high risk. Land use classes were then tabulated against vulnerability risk classes using a spatial join constraint: very low vulnerability resulted associated with areas not subject to intensive agrochemical inputs such as forest, to unutilized areas and to fruit tree orchards; fruit and vegetables together with olive orchards and cereals classes showed instead an average medium risk; finally grape orchards and grassland/pasture land showed to be associated with high risk (figure 4).

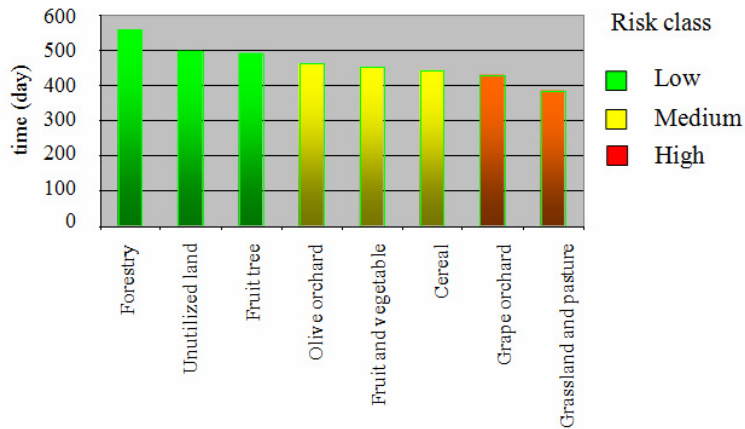


Fig.4. Vulnerability risk for Land Use Classes.

Spatial distribution, fragmentation and perimeter to area ratio of land use patches, were taken into account to ensure data homogeneity during generalization of travel times and subsequently land use class risk rankings [32]. It should be considered that the results illustrated herein refer to a conservative and nonreactive solute. Anyway, such results can be easily extended to the case of reactive transport by using the following expression:

$$f(I) = \frac{1}{R} \frac{1}{\sqrt{2\pi}\sigma_{ef}\left(\frac{I}{R}\right)} \exp\left[-\frac{(\ln I/R - \mu_{ef})^2}{2\sigma_{ef}^2}\right] \exp(-k_{dr}t) \quad (8)$$

where R is the retardation coefficient, which can be assumed to vary with depth and k_{dr} is the first-order decay rate of the solute. Both the parameters can be considered either deterministic or be randomly generated, depending also on the available data.

The results can be also extended to any input at the surface by convolving the 80 cm upscaled pdf with the solute input (see equation 3).

5. Conclusions

The main characteristic of this study was that it considered the integrated effects of spatial variation of soil profiles, and related soil physical properties, both in the vertical and horizontal dimensions. This is the main strength of the approach, as many previous studies mainly focused mainly on the horizontal direction only. Anyway, this was not a simple task, because of the relatively sparse profile data and the complexity of the spatial variation in the vertical direction.

The over goal of this study, then, was developing of a regional-scale simulation approach for vadose zone leaching relying on easily available and accessible data, on affordable computational efforts, and providing quantitative answers to ground water vulnerability to agrochemical leaching at regional scale within a defined confidence interval. It showed to be a useful and practical tool for assessing ground water vulnerability to NPS pollution at regional scale in that it uses publicly available data and demands reasonable computational efforts still ensuring good data accuracy levels, especially if compared to those qualitative models that although being the most common solution for regional studies, they rely uniquely on empirical conceptualizations of chemical leaching processes and give as outputs only general qualitative indication rankings without quantification of risk in terms of travel times.

The stochastic approach used herein considers the field soil as an ensemble of parallel and statistically independent tubes, assuming only vertical flow. The stream tubes approach is generally used in a probabilistic framework. Each stream tube defines local flow properties that are assumed to vary randomly between the different stream tubes. Accordingly, the strength of the stochastic framework we used lies in the uncertainty information of the estimated travel times.

Land use and agronomic inputs can be closely monitored in regard to ground water vulnerability of their locations using the outputs of this methodology; this result can indeed support land use decision makers in activity planning and resource management of rural areas in respect of environmental protection. Development of accurate studies of this nature at regional, basin and sub-basin scales will greatly benefit from founding of soil data survey and collection programs at public agencies level.

References

- [1] Corwin DL. GIS applications of deterministic solute transport models for regional-scale assessment of non-point source pollutants in the vadose zone. In D. L. Corwin and K. Loague (eds.) *Applications of GIS to the Modeling of Non-Point Source Pollutants in the Vadose Zone*. Soil Science Society of America, Madison, WI; 1996; p. 69-100.
- [2] Comegna V, Coppola A, Sommella A. Nonreactive solute transport in variously structured soil materials as determined by laboratory-based time domain reflectometry (TDR) *Geoderma*. 1999;**92**:167–184.
- [3] Jury W, Roth K. *Transfer Functions and Solute Movement Through Soil: Theory and Applications* Birkhäuser, Basel, 1990; p 235.
- [4] Comegna V, Coppola A, Sommella A. Effectiveness of equilibrium and physical non-equilibrium approaches for interpreting solute transport through undisturbed soil columns. *J. Contam. Hydrol.* 2001;**50**:121–138.
- [5] Beven K, Germann P. Macropores and water flow in soils. *Water Resour. Res.* 1982;**18**:1311-1325.
- [6] Coppola A, Gerke HH, Comegna A, Basile A, Comegna V. Dual-permeability model for flow in shrinking soil with dominant horizontal deformation. *Water Resour. Res.* 2012, **48**:W08527, doi:10.1029/2011WR011376.
- [7] Keller AA, Sirivithayapakorn S. Transport of colloids in unsaturated porous media: Explaining large scale behavior based on pore scale mechanisms. *Water Resour. Res.* 2004;**40**:W12403, doi:10.1029/2004WR003315.
- [8] Flury M, Qiu H. Modeling colloid-facilitated contaminant transport in the vadose zone. *Vadose Zone J.* 2008;**7**: 682–697.
- [9] Vogel HJ, Roth K. Moving through scales of flow and transport in soil. *J. Hydrol.* 2003;**272**:95–106.
- [10] Woods SA, Kachanoski RG, Dyck MF. Long-Term Solute Transport under Semi-Arid Conditions: Pedon to Field Scale. *Vadose Zone J.* 2006;**5**:365–376.
- [11] Comegna A, Coppola A, Comegna V, Severino G, Sommella A, Vitale CD. State space approach to evaluate spatial variability of field measured soil water status along a line transect in a volcanic-vesuvian soil. *Hydrol Earth Syst Sc* 2010;**14**:2455-2463.
- [12] Severino G, Comegna A, Coppola A, Sommella A, Santini A. Stochastic analysis of a field-scale unsaturated transport experiment. *Adv. Water Resour. Research* 2010;**33**:1188-1198.
- [13] Coppola A, Comegna A, Dragonetti G, Dyck M, Basile A, Lamaddalena N, Kassab M, Comegna V. Solute transport scales in an unsaturated stony-soil. *Adv. Water Resour.* 2011;**34**:747-759.
- [14] Corwin DL, Loague K, Ellsworth TR. Modeling nonpoint source pollutants in the vadose zone with GIS. *Environmental Science and Technology* 1997;**31**(8):2157–2175.
- [15] Stewart IT, Loague K. Development of type transfer function for regional scale nonpoint source groundwater vulnerability assessment. *Water Resour. Res.* 2003;**39**:1-13.
- [16] Stewart IT. *Development of a type transfer function approach for modeling non-point-source vadose-zone pesticide leaching at the regional scale*, Ph.D. thesis, Stanford Univ., Stanford, Calif., 2001.
- [17] Wösten JHM, Pachepsky YA, Rawls WJ. Pedotransfer functions: Bridging the gap between available basic soil data and missing soil hydraulic characteristics. *J. Hydrol.* 2001;**251**:123–150.
- [18] Vereecken H, Weynants M, Javaux M, Pachepsky Y, Schaap M G, van Genuchten M.Th. Using pedotransfer functions to estimate the van Genuchten–Mmuaem soil hydraulic properties: A review. *Vadose Zone J.* 2010;**9**:1–26.
- [19] Kay BD, da Silva AP, Baldock JA. Sensitivity of soil structure to changes in organic carbon content: Predictions using pedotransfer functions. *Can. J. Soil Sci.* 1997;**77**:655-667.
- [20] Tomasella J, Hodnett MG. Estimating soil water retention characteristics from limited data in Brazilian Amazonia. *Soil Sci.* 1998,**163**:190–202.
- [21] van Genuchten MTh. A closed-form equation for predicting the hydraulic conductivity of unsaturated soils. *Soil Sci. Soc. Am. J.* 1980;**44**:892-898.

- [22] Mualem Y. A new model for predicting the hydraulic conductivity of unsaturated porous media, *Water Resour. Res.* 1976;**12**:513-522.
- [23] Arya LM, Paris JF. A physicoempirical model to predict the soil moisture characteristic from particle-size distribution and bulk density data. *Soil Sci. Soc. Am. J.* 1981;**45**:1023–1030.
- [24] Basile A, D'Urso G. Experimental corrections of simplified methods for predicting water retention curves in clay-loamy soils from particle-size determination. *Soil Technol.* 1997;**10**:261–272.
- [25] Arya LM, Leij FJ, van Genuchten MTh, Shouse PJ. Scaling parameter to predict the soil water characteristic from particle-size distribution data. *Soil Sci. Soc. Am. J.* 1999a;**63**:510–519.
- [26] Arya LM, Leij FJ, Shouse PJ, van Genuchten MTh. Relationship between the hydraulic conductivity function and the particle-size distribution. *Soil Sci. Soc. Am. J.* 1999b;**63**:1063–1070.
- [27] Carsel RF, Parrish RS. Developing joint probability distributions of soil water retention characteristics, *Water Resour. Res.* 1988;**24**(5):755-769.
- [28] Smith RE, Diekkruger B. Effective soil water characteristics and ensemble soil water profile in heterogeneous soils. *Water Resour. Res.* 1996;**32**:1993–2002.
- [29] Scotter DR, Ross PJ. The upper limit of solute dispersion and soil hydraulic properties. *Soil Sci. Soc. Am. J.* 1994;**58**:659–663.
- [30] Hamlen CJ, Kachanoski RG. Field solute transport across a soil horizon boundary. *Soil Sci. Soc. Am. J.* 1992;**56**:1716–1720.